EQCNN: Enhanced Remote Sensing Imagery Classification with Circuit-Based Error-Corrected Quantum Convolutional Neural Networks

Muhammad Zaman
Faculty of Computer Science,
University of Lahore,
Sargodha, Punjab 40100, Pakistan
mzamancui@gmail.com

Tanzila Kehkashan
Faculty of Computing,
Universiti Teknologi Malaysia,
Johor Bahru, Malaysia
tanzila.kehkashan@gmail.com

Adnan Akhunzada
College of Computing & IT,
Department of Data and Cybersecurity,
University of Doha for Science & Technology,
Doha, Qatar
adnan.adnan@udst.edu.qa

Hashem Alaidaros
Department of Cybersecurity,
Dar Al-Hekma University,
Jeddah, Saudi Arabia
haidarous@dah.edu.sa

Mueen Uddin
College of Computing & IT,
Department of Data and Cybersecurity,
University of Doha for Science & Technology,
Doha, Qatar
mueen.uddin@udst.edu.qa

Muhammad Azeem
Faculty of Computer Science,
University of Lahore,
Sargodha, Punjab 40100, Pakistan
azeem31570@gmail.com

2024 International Conference on Digital Image Computing: Techniques and Applications (DICTA) | 979-8-3503-7903-7/24/$31.00 ©2024 IEEE | DOI: 10.1109/DICTA63115.2024.00109

Abstract

Quantum information processing is more complex than classical counterpart because of the No-Cloning theorem, decoherence, and issues detecting quantum states. Building a quantum computer without error detection and correction module is challenging. To overcome this challenge, qubit error correction codes are implemented. Inadequate error detection and correction codes have been the downfall of earlier attempts to encode quantum information, leading to disrupted qubit transmission. Qubit information is decohered by circuit noise. Unfortunately, the principal qubit error, phase flip error is not corrected by existing qubit error correction methods. In this study, we proposed Quantum Error Detection and Correction scheme (QEDC) to keep qubit in a coherent state. Used S gates, unitary gates, 10 CNOT gates, and Hadamard gates spanning on 4 physical and 1 logical qubits over the IBM Quantum Experience Machine. We found that the error probability is reduced to 7.91% owing to the efficiency of the quantum information encoding and phase flip control. Furthermore, we proposed Error Corrected Quantum Convolution Neural Network (EQCNN) for Image Classification. EQCNN combat and correct qubit errors that occur during the image processing. EQCNN outperformed over Earth Observatory (EO) dataset, EuroSAT and achieved an impressive results of 99.3% accuracy, 98.9% F1-score, 96.73% precision, and 98.4% recall.

I. Introduction

Quantum computing can solve essential physical processes, optimize intricate cost functions, and bring novel image processing problems that classical computers cannot perform [6]. However, practical quantum components fail quite often, making these aims unattainable. These applications need quantum mechanics based error correction systems. Quantum error correction codes safeguard entangled data by converting a few physical qubits into logical ones [44]. Fault-tolerant (FT) technologies, which control system error, are also needed [46].The absence of

979-8-3503-7903-7/24/$31.00 ©2024 IEEE
DOI 10.1109/DICTA63115.2024.00109

fault-tolerant techniques may result in the occurrence of errors at critical circuit nodes, leading to logical errors that ultimately render error correction ineffective.

Four qubit error detection codes exhibit FT state preparation and detection[35]. These algorithms can detect problems but cannot extract enough data to solve them. Classical repetition codes may correct one dimensional quantum errors in quantum systems [20], [52], [31]. Qubits were encoded in error correction code at early stage. The encoding technique was not fault-tolerant, and the circuit was too tiny to quantify error syndromes non-destructively using ancilla [42], [43]. Parallel bosonic codes have exhibited decoded operations and FT detection on encoded qubit [45], [36], [7]. Both 4 qubit and bosonic codes must provide a FT state that fixes all single qubit errors. Quantum states are fragile, so making errors are more probable. Quantum states that are not completely understood are vulnerable to measurement errors and data loss[10], [11].

The No-Cloning theorem prevents error correction algorithms from accounting for quantum states [37]. Firstly, Repetition codes revealed the qubit error. Three qubits constitute a single qubit code since they repeat. If the input is a $\|0\rangle$, the encoded value will be $\|000\rangle$, and if it is a $\|1\rangle$, the encoded value will be $\|111\rangle$. Most of the qubits will be analyzed to locate the error. In such case when the received information is $\|001\rangle$, the third qubit was the source of the error, and the true value of that qubit is $\|0\rangle$ because $\|1\rangle$ and $\|0\rangle$ are mutually exclusive. This method cannot identify errors if two qubits are changed. it requires nine qubits to discover and correct a random error in a single qubit and Repetition is altered. More than fifty qubits can simulate and compute synchronously.

The selected Quantum Convolutional Neural Network (QCNN) is distinct from CNNs in a way that it incorporates a quantum layer into the neural network [39]. Multiple gate based circuits have been compared to the hybrid QCNN when assessing its multi class identification and processing efficiency in Land use and land cover (LULC) classification applications [13]. While QCNNs employing CNN with a quantum circuit do extremely well on EO image classification [18]. They still can not stop quantum errors from corrupting the quantum data as it travels through the circuit . Efforts to manipulate data with qubits have been persistently inhibited by the challenges arising from the loss of coherence since their inception.

In this article, Quantum error detection and correction approach for quantum systems is developed, which is subsequently implemented using various QCNN to manage quantum errors while processing image input. The EO dataset is used for the image classification[32], [41]. In particular, many quantum circuits will be applied to the problem of image classification for EO images, and the results will be compared in terms of both accuracy and precision along with recall and F1 Score [51], [16].

The Main contribution of this research work reside in:

- Various quantum error correction (QEC) codes have been examined in our investigation.
- The construction of a qubit error detection and correction mechanism was undertaken.
- The proposed quantum convolutional neural network with error correction is presented.
- Experimented the proposed model over referenced EO dataset EuroSAT [21].

Here, it is important to note that the quantum error detection and correction system is developed and designed from scratch using an entirely innovative encoding approach. During this procedure, 872 experiments were conducted using the Quantum Experience Machine in a long-term experimental configuration. Many distinct configurations of quantum gates have been taken into account in the experimental setup. Furthur, QEDC is implemented with QCNN to proposed novel EQCNN which enable error free iamge processing. EQCNN is deployed to performed experimentation over EO dataset, whcih cameup with excellent results to prove the efficacy of EQCNN.

II. Related Work

Quantum computing researchers are prioritizing program development for noisy intermediate-scale quantum devices. Quantum computers cannot fulfill their potential without FT quantum computing[2]. Qubit error correction and FT have been studied using Nuclear magnetic resonance (NMR) trapped ions, photonics, Nitrogen vacancy (NV) centers, and superconducting circuits [49]. Biswal $et\ al.$ construct T-Depth, auxiliary cost, and T-Count for a majority-based one-bit and n-bit Full Adder (FA) for fault-tolerant quantum logic circuits[12]. Carlos $et\ al.$ evaluate Reed Solomon and Bose-Chaudhuri-Hocquenghem (BCH) based quantum error correcting code for entanglement using the Hermitian metric [22]. Andrew $et\ al.$ argued that Shor-Laflamme weight enumerators of codeword stabilized quantum codes might be distant enumerators to a comparable classical code [34].

Hybrid quantum-classical methodologies derived from the category of variational quantum algorithms were initially proposed within the domain of chemistry [8]. These approaches have more recently garnered attention for their potential in addressing diverse machine learning objectives on Noisy Intermediate-Scale Quantum (NISQ) devices[29]. Examples of such objectives include classification graph embedding and the approximation of the deep Q-value function in reinforcement learning scenarios[25].

Robert $et\ al.$ introduce block perfect tensors to the holographical quantum error correction coding class [34].

Many holographic codes are feasible without this restriction. The self dual Calderbank Shor Steane (CSS) heptagonal holographical code, developed from 7 qubit steane code, demonstrates this [5]. Finally, apply a simple, optimal erasur decoder to the heptagon code and compare to other holographical codes to show the optimal threshold for erasur passing [30].

Debjit *et al.* demonstrate Non-destructive Greenberger-Horne-Zeilinger (GHZ) state discrimination and automatic error correction using an IBM 5-qubit quantum computer [47]. For error correction, Mummadi *et al.* proposed a noval encoding strategy whereby 5 qubits are used to protect a single qubit of information from a single random error but disregarded entanglement when encoding qubits and cycling the circuit [8]. The encoding approach is shown to be ineffective due to entanglement loss.

According to Vojtech *et al.* machine learning with quantum computing revolutionized computation and tackle previously intractable problems [17]. Chen *et al.* propose layer-quantum neural networks where all quantum gates are unitary and linear, non-linearity in QNNLs is the biggest issue [24]. Muller *et al.* improve the encoding method for a quantum error correcting code with few bits and unexpected but continuous phase variations [9].

While quantum computing has made great strides, many algorithms still cannot be run on commercially available quantum hardware[26]. Classification algorithms based on circuits are insufficient for EO images [33]. Now that a Quantum Annealer (QA) based variant of the CNN has shown performance on par with the original CNN, QA is expected to replace CNN as the method of choice for practical EO image classification [27].

Since the 1990s, Earth observation imagery has been used to classify LULC for the purposes of ensuring the availability of natural resources, tracking consumption, and developing growth strategies [19]. Through its role in delivering up-to-date and comprehensive information on earth condition, LULC classification has a significant impact on the atmosphere, soil corrosion, water reservoir, and biological deposits, and is indirectly related to global environmental concerns [28].

Numerous research have been undertaken to examine the efficacy and efficiency of various classifiers [4], [3]. Nevertheless, the majority of these research have mostly used pixel based methodologies [23], [1]. The prevalence of object based methodologies has sparked a growing fascination in the comparative analysis of various machine learning classifiers via object-based techniques [15], [50], [38].

Denny *et al.* suggested convolutional neural network inspired by quantum-classical image classification system referred as quanvolutional neural network (QNN) [48]. Alam *et al.* suggested a quantization, boosting, and QNN

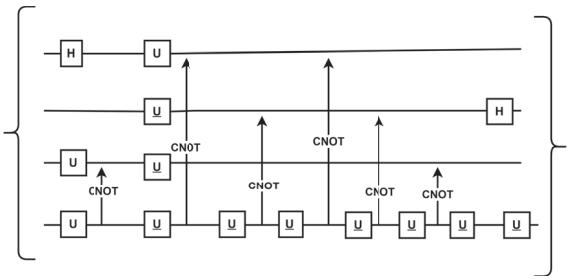

Fig. 1. Qubit Information Encoding Circuit

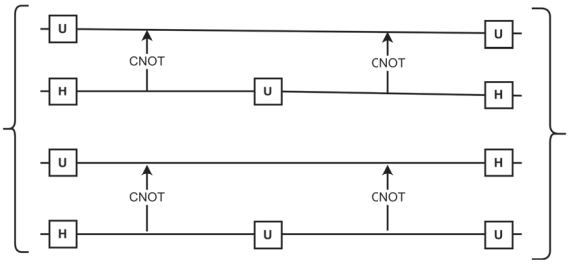

Fig. 2. Qubit Error detection and correction Circuit

full-stack QML image classifier where QNN training uses PCA/CAE image characteristics [14]. Alessandro *et al.* investigate at hybrid circuit-based QCNNs for image classification in remote sensing[40].

III. QEDC Scheme

A unique combination of Unitary gates are used to encode the information into the quantum system. Hadamard gate oversee the bit flip, with the unitary gate over $\pi/4$ angle after making phase shift keep the precious quantum data secured from errors to be happened. As the data is encoded through unitary gate $\pi/4$ and passed to CNOT gate iteratively, each qubit passed through gates which keep the qubit information error free. If the error occur during the gates operations, it detects very efficiently and correct it during operation. Hadamard gate keep it safe from bit flip, even if it happens, correction is performed.

Qubit information encoding mechanism, as shown in **Figure** 1 made the circuit more secure against the probability of error to occurr in the data. As the qubits shots are fed to circuit the unitary gates along with Hadamard and CNOT preserve the state and phase flip. $\pi/4$ phase shift is carried by unitary gate which make it more secure for phase flip. Hadamard gate along the circuit preserve the bit flip error. Certainly, take that long care and secure circuit, there is still some noise present in the circuit which cause the error to happen along the circuit, so the error detection and correction mechanism, shown in **Figure** 2 detects and corrects the errors to make the qubits coherent while processing.

It is the simplest structure for error detection and

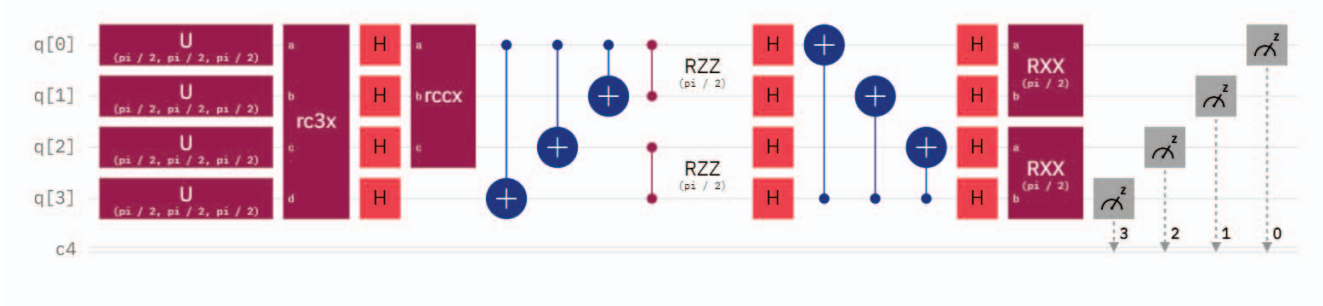

Fig. 3. Qubit error detection and correction circuit

correction with 4 physical qubits be charged with one logical qubit over the circuit with, multiple unitary gates with the angle of $\pi/4$, 10 CNOT gates and Hadamard gates to control the rotation along the axis as shown in **Figure** 3. A phase disk is appended to the very end of each string of quantum registers in order to offer a live display of the phase shift in real time as well as the possibility to change the angle of shift. This was done so that the user may monitor the phase shift in real time. The state of a single qubit may be described in the following manner (Eq: 1):

$$\psi = \sqrt{1-p}\|0\rangle + e^{j\phi}\sqrt{p}\|1\rangle \tag{1}$$

where "p" is the probability that the qubit is in the $\|1\rangle$ state and ψ is the quantum phase. In many aspects, the value 'p' is similar to the classical probabilistic bit When p = 0, the qubit is in the $\|0\rangle$ state; when 'p' = 1, it is in the $\|1\rangle$ state; and when 'p' = $1/2$, it is in the $50/50$ mixed state. It is termed a superposition because, unlike ordinary bits, this combination may have a quantum phase.

IV. Experimental Results for QEDC

A. Probability of Error

Due to efficient quantum information encoding, the probability of error is reduced to 7.91%. The qubit error detection and correction scheme with S, unitary, and 10 CNOT gates in addition to Hadamard gates over 4 physical and 1 logical qubit implemented on the IBM Quantum Experience Machine, results shown in **Figure** 4.

The previous method, implemented with IBM Quantum Experience Machine, used a major count of S, unitary, and 4 CNOT gates over 5 physical and 1 logical qubit; nevertheless, the probability of error is 56.25% in 1024 shots owing to an effect regarded as phase flip being ignore while qubit encoding. During the course of experimentation, 872 simulation are performed on different IBM Systems and Simulators. Every simulations environment has different qubit handling capacities like wise,

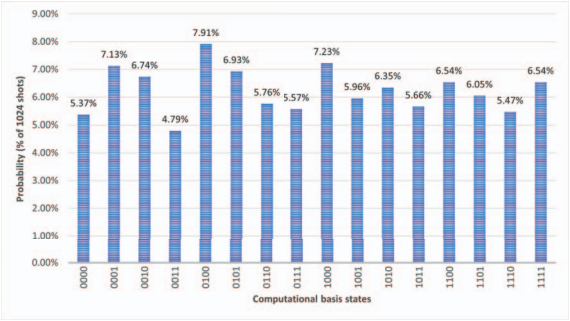

Fig. 4. Probability of Error detected and corrected along the circuit.

ibmq_qasm_simulator is 32 qubit. Capacities may vary over the qubit architecture. Qubit error detection and correction scheme is also deployed over logical quantum computers where the efficiency for the QEDC code is tested for the future quantum computers. So, the Logical Quantum Computer though give the same results for the QEDC over the constant experimentation setup as the simulator.

B. Quantum Magnitude

The quantum amplitudes are shown in the form of a bar chart on this page. The computational basis states are shown running along the bottom axis. Each computational base state is represented by a vertically oriented amplitude. This amplitude is shown in a horizontal position. The color of bar represent the phase angle. The graph represents the quantum phase $3\pi/2$ associated with that color shown in **Figure** 5.

C. Q-Sphere

The q-sphere depict the angle be $3\pi/2$ along with the state vector $\|1001\rangle$ as in **Figure** 6. In contrast, a Q-sphere is one-of-a-kind and irreplaceable. Transition between two or more (up to five) qubit states is represented by this symbol. A $\|0000\rangle$ Q-ball is in pristine condition, whereas a $\|1111\rangle$ ball is in worst condition.

TABLE I. Performance of Circuit based error detection and correction Scheme

Circuit Parameter			Error Probability		
V.Seed	Basis State	Phase Angle	max	avg	min
6000	$\|0101\rangle$	π	7.81%	6.54%	4.88%
5000	$\|1001\rangle$	$3\pi/2$	**7.9%**	**6.25%**	**4.78%**
4000	$\|0101\rangle$	π	7.99%	6.66%	4.88%

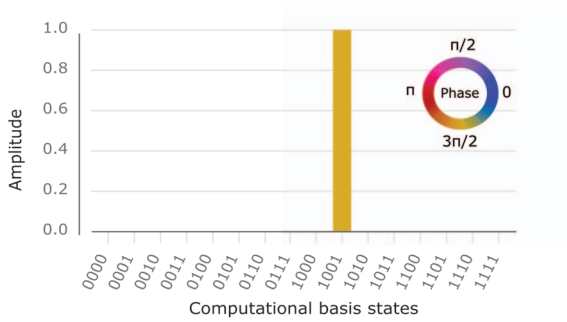

Fig. 5. Quantum Magnitude of State vector on phase angle of $3\pi/2$.

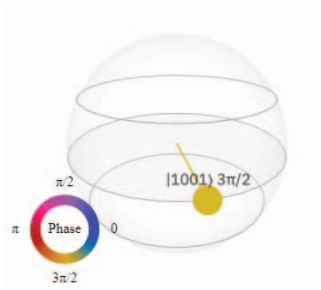

Fig. 6. Q-Sphere with State vector over the Phase angle $3\pi/2$.

D.Comparison against benchmark QEC Codes

We have made a certain comparison of existing QEC codes and Proposed Error Detection and Correction Scheme where certain measures are considered for comparison purpose. Novel Encoding Quantum Error Correction (NEQEC) with the basis state $\|11111\rangle$ with 5 physical qubits has an angle of $\pi/2$ acquired the error probability score of 56.25%, which is the major setback to quantum circuit for handling qubit coherence. Proposed qubit error detection and correction has performed excellent with basis state $\|1001\rangle$ over the angle of $3\pi/2$ with the error probability of just 7.71% mention in **Table** IV-D. The novel quantum information encoding scheme helped the circuit to handle the qubit coherence at maximum and the rest error occurred in the circuit was detected and corrected by the QEDC circuit.

If a shift in phase happens during data transmission, it may be identified using the following equation and a phase measurement (Eq:2).

$$Phase\ measurement = \sqrt{1-p_r}\|\gamma\rangle\ + e^{iP_h}\sqrt{p_r}\|\tau\rangle \quad (2)$$

This equation is used to calculate the phase angle of quantum states $\|\gamma\rangle$, $\|\tau\rangle$ with the probability p_r at the time t with phase P_h. For input states $\|0\rangle$ & $\|1\rangle$, the equation will be modified as $\sqrt{1-p_r}\|0\rangle+\sqrt{p_r}\|1\rangle$. The probability error rate is computed by using such formula $M(p_r) - E(p_r)$.

V. Dataset

Research analyzes 27,000 geo-referenced and labeled images from the EuroSAT dataset [21], based on Sentinel-2 satellite imagery, covering 13 spectral bands and 10 classifications. Sentinel-2 consists of two satellites, Seninel-2A and Sentinel-2B, which together provide near-complete Earth coverage every five days with a spatial resolution of up to 10 meters per pixel. The images highlight similarities and differences across various classes, such as agricultural and natural land covers.

VI. EQCNN for image classification

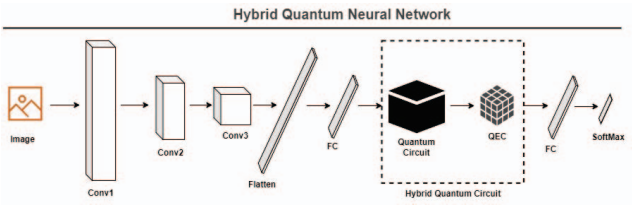

Fig. 7. Proposed Model for EQCNN

We propose an Error Corrected Quantum Convolutional Neural Network (EQCNN) that utilizes a quantum circuit for classification, with an error correction code to maintain qubit coherence. The model converts 1 logical qubit of information into 4 quantum bits, employing CNOT, S, and unitary operations at an angle of $\pi/4$ for efficient encoding. To implement this hybrid QCNN with qubit error correction, two distinct quantum circuits were designed, using four qubits instead of fewer. These circuits employ entangled qubits and Hadamard gates to create a superposition state, followed by Ry gate rotations to

TABLE II. Comparison table between Existing QEC codes and Proposed Error Detection and correction Scheme

Model	Circuit Parameter		Error Probability		
	Basis State	Phase Angle	max	avg	min
NEQEC	$\|11111\rangle$	$\pi/2$	56.25%	50%	43.75%
AEC	$\|0101\rangle$	π	54.8%	51.66%	46.48%
QEDC	$\|1001\rangle$	$3\pi/2$	**7.71%**	**6.25%**	**4.68%**

1. NEQEC work for error correction with 5-qubits and $\pi/2$ Phase angle.
2. Automated Error correction code with π Phase angle to correct the qubit errors.
3. Novel Proposed QEDC work with 4-qubits to detect and correct qubit error with $3\pi/2$ Phase angle

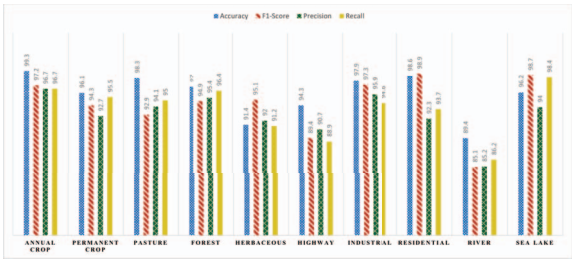

Fig. 8. EQCNN implemented with Earth Observatory referenced EuroSAT dataset and attain the accuracy, f1-score, precision, recall to 99.3%, 98.9%, 96.7%, 98.4% respectively.

achieve quantum node activation, optimizing classification performance through matrix multiplication and tensor products of the gates.

The QCNN architecture includes a classical component based on a modified CNN, adjusted for the input image size of the EuroSAT dataset used in image classification. Unlike the original CNN, this model features two fully connected layers, one of which is a quantum layer, to accommodate the required number of input classes and output sizes. This integration of quantum and classical components is intended to enhance the overall performance and efficiency of the neural network in handling complex data, particularly in applications involving Earth observation imagery.

A.Comparison analysis with benchmark studies

The proposed Quantum Convolutional Neural Network (QCNN) classifier was compared against two versions of classical classifiers: one using a fully connected layer with 16 nodes, and another employing a multi-layer perceptron with layers containing 10, 32, 64, and 256 nodes. Both classifiers were evaluated on the EuroSAT dataset, which consists of 27,000 annotated images from the Sentinel-2 satellite, covering 10 classes and 13 spectral bands. The dataset was split 80/20 for training and validation. Three different quantum circuits were tested, including an error-corrected QCNN, to explore their performance on image classification tasks. All models were developed from scratch, with hyperparameters and loss functions tailored to the dataset's specific requirements, and trained on Google Colaboratory using a Tesla K80 GPU.

The QCNN models were trained for 50 epochs with the Adam optimizer and a learning rate of 0.0002, while the classical models required around 100 epochs to converge. Both quantum and classical models used a backpropagation-based training approach, with data fed into both the CNN and Quantum Circuit, followed by weight adjustments based on error gradients. The validation results demonstrated that the quantum models, especially those using entangled qubits with an error correction scheme, significantly outperformed the classical models. The EQCNN achieved outstanding performance with an accuracy of 99.3%, an F1-score of 98.9%, precision of 96.7%, and recall of 98.4% respectively **Figure** 8. These results suggest that the choice of quantum circuits is crucial not only for the specific application but also for managing the complexity of the data and maintaining qubit coherence during processing.

VII. Conclusion

We propose a circuit-based error detection and correction scheme for quantum systems, utilizing unitary, Hadamard, and CNOT gates to encode qubit data while preserving coherence with a $3\pi/2$ angle shift over the basis state $\|1001\rangle$. The scheme detects and corrects errors using logical qubits, offering significant advancements in quantum computing, particularly in quantum machine learning. This method is applied to a Quantum Convolutional Neural Network (QCNN) to create an Error Corrected QCNN (EQCNN) for image classification on the EuroSAT dataset. The model achieved exceptional results, with 99.3% accuracy, 98.9% F1-score, 96.7% precision, and 98.4% recall, demonstrating its effectiveness for real-world image classification tasks and its potential applicability across various types of complex image classification problems. Adaptability and efficiency on larger quantum platforms remain areas for further investigation to ensure its viability.

References

[1] T. Adugna, W. Xu, and J. Fan. Comparison of random forest and support vector machine classifiers for regional land cover mapping

TABLE III. Performance Comparison of Different Models

Model	Dataset	Accuracy	Precision	Recall	F1-Score
SVM [48]	UAS Data	73	75	71	72
3DQConv [51]	Houston Data	91	90	89	92
ANN [38]	LandSat-8	98	97	93	94
QCNN [40]	EuroSAT	99	95	94	95
EQCNN	EuroSAT	**99.3**	96.73	**98.4**	**98.9**

using coarse resolution fy-3c images. *Remote Sensing*, 14(3):574, 2022. 3

[2] M. Alam, S. Kundu, R. O. Topaloglu, and S. Ghosh. Quantum-Classical hybrid machine learning for image classification (ICCAD special session paper). In *2021 IEEE/ACM International Conference On Computer Aided Design (ICCAD)*, pages 1–7, Nov. 2021. 2

[3] A. Alekseev, D. Chernikhovskii, L. Vetrov, M. Gurjanov, and I. Nikiforchin. Determination of the state of forests based on a regular grid of ground-based sample plots and sentinel-2b satellite imagery using the k-nn ("nearest neighbor") method. In *IOP Conference Series: Earth and Environmental Science*, volume 876, page 012002. IOP Publishing, 2021. 3

[4] S. Amini, M. Saber, H. Rabiei-Dastjerdi, and S. Homayouni. Urban land use and land cover change analysis using random forest classification of landsat time series. *Remote Sensing*, 14(11):2654, 2022. 3

[5] L. Berent, T. Hillmann, J. Eisert, R. Wille, and J. Roffe. Analog information decoding of bosonic quantum low-density parity-check codes. *PRX Quantum*, 5(2):020349, 2024. 3

[6] L. Biswal, B. Mondal, A. Chakraborty, and H. Rahaman. Efficient quantum implementation of majority-based full adder circuit using Clifford+T-group. In *Lecture Notes in Electrical Engineering*, Lecture notes in electrical engineering, pages 53–63. Springer Singapore, Singapore, 2022. 1

[7] W. Cai, Y. Ma, W. Wang, C.-L. Zou, and L. Sun. Bosonic quantum error correction codes in superconducting quantum circuits. *Fundamental Research*, 1(1):50–67, 2021. 2

[8] A. Callison and N. Chancellor. Hybrid quantum-classical algorithms in the noisy intermediate-scale quantum era and beyond. *Physical Review A*, 106(1):010101, 2022. 2, 3

[9] G. Chen, S. Long, Z. Yuan, W. Li, and J. Peng. Robustness and explainability of image classification based on qcnn. *Quantum Engineering*, 2023(1):2842217, 2023. 3

[10] Y.-A. Chen, A. V. Gorshkov, and Y. Xu. Error-correcting codes for fermionic quantum simulation. *SciPost Physics*, 16(1):033, 2024. 2

[11] J. Del Pino and O. Zilberberg. Dynamical gauge fields with bosonic codes. *Physical Review Letters*, 130(17):171901, 2023. 2

[12] A. Delilbasic, G. Cavallaro, M. Willsch, F. Melgani, M. Riedel, and K. Michielsen. Quantum support vector machine algorithms for remote sensing data classification. In *2021 IEEE International Geoscience and Remote Sensing Symposium IGARSS*, pages 2608–2611, July 2021. 2

[13] M. Digra, R. Dhir, and N. Sharma. Land use land cover classification of remote sensing images based on the deep learning approaches: a statistical analysis and review. *Arabian Journal of Geosciences*, 15(10):1003, 2022. 2

[14] M. Dixit, K. Chaurasia, and V. K. Mishra. Dilated-resunet: A novel deep learning architecture for building extraction from medium resolution multi-spectral satellite imagery. *Expert Systems with Applications*, 184:115530, 2021. 3

[15] Q. V. V. Du, T. M. Pham, H. D. Nguyen, Q. H. Nguyen, V. T. Pham, H. C. Nguyen, et al. An experimental comparison of pixel-based and object-based classifications with different machine learning algorithms in landscape pattern analysis–case study from quang ngai city, vietnam. In *IOP Conference Series: Earth and Environmental Science*, volume 1345, page 012019. IOP Publishing, 2024. 3

[16] F. Fan, Y. Shi, and X. X. Zhu. Urban land cover classification from sentinel-2 images with quantum-classical network. In *2023 Joint Urban Remote Sensing Event (JURSE)*, pages 1–4. IEEE, 2023. 2

[17] V. Frants, S. Agaian, and K. Panetta. Qcnn-h: Single-image dehazing using quaternion neural networks. *IEEE Transactions on Cybernetics*, 53(9):5448–5458, 2023. 3

[18] S. Gaur and R. Singh. A comprehensive review on land use/land cover (lulc) change modeling for urban development: current status and future prospects. *Sustainability*, 15(2):903, 2023. 2

[19] P. R. Giri, M. Kurokawa, and K. Saito. Quantum negative sampling strategy for knowledge graph embedding with variational circuit. In *2023 IEEE International Conference on Quantum Computing and Engineering (QCE)*, volume 2, pages 280–281. IEEE, 2023. 3

[20] J. M. Günther, F. Tacchino, J. R. Wootton, I. Tavernelli, and P. K. Barkoutsos. Improving readout in quantum simulations with repetition codes. *Quantum Science and Technology*, 7(1):015009, 2021. 2

[21] P. Helber, B. Bischke, A. Dengel, and D. Borth. Eurosat: A novel dataset and deep learning benchmark for land use and land cover classification. *IEEE Journal of Selected Topics in Applied Earth Observations and Remote Sensing*, 12(7):2217–2226, 2019. 2, 5

[22] C. C. HOONG. *CONTROL AND MANIPULATION OF SINGLE ATOMS FOR INTERFACING WITH LIGHT*. PhD thesis, University of Basel, 2023. 2

[23] X. Hu, P. Zhang, Q. Zhang, and J. Wang. Improving wetland cover classification using artificial neural networks with ensemble techniques. *GIScience & Remote Sensing*, 58(4):603–623, 2021. 3

[24] W. Hua, C. Zhang, W. Xie, and X. Jin. Polarimetric sar image classification based on ensemble dual-branch cnn and superpixel algorithm. *IEEE Journal of Selected Topics in Applied Earth Observations and Remote Sensing*, 15:2759–2772, 2022. 3

[25] T. Hur, L. Kim, and D. K. Park. Quantum convolutional neural network for classical data classification. *Quantum Machine Intelligence*, 4(1):3, 2022. 2

[26] T. Hur, L. Kim, and D. K. Park. Quantum convolutional neural network for classical data classification. *Quantum Machine Intelligence*, 4(1):3, 2022. 3

[27] S. Hussain, M. Mubeen, and S. Karuppannan. Land use and land cover (lulc) change analysis using tm, etm+ and oli landsat images in district of okara, punjab, pakistan. *Physics and Chemistry of the Earth, Parts a/b/c*, 126:103117, 2022. 3

[28] Y.-K. Kim, I. Baek, K.-M. Lee, J. Qin, G. Kim, B. K. Shin, D. E. Chan, T. J. Herrman, S.-k. Cho, and M. S. Kim. Investigation of reflectance, fluorescence, and raman hyperspectral imaging techniques for rapid detection of aflatoxins in ground maize. *Food Control*, 132:108479, 2022. 3

[29] D. Lee, J. Lee, S. Hong, H.-T. Lim, Y.-W. Cho, S.-W. Han, H. Shin, J. ur Rehman, and Y.-S. Kim. Error-mitigated photonic variational quantum eigensolver using a single-photon ququart. *Optica*, 9(1):88–95, 2022. 2

[30] P.-Z. Li, J. Dias, W. J. Munro, P. van Loock, K. Nemoto, and N. Lo Piparo. Performance of rotation-symmetric bosonic codes in a quantum repeater network. *Advanced Quantum Technologies*, page 2300252, 2024. 3

[31] M. Liepelt, T. Peduzzi, and J. Wootton. Enhanced repetition codes for the cross-platform comparison of progress towards fault-tolerance. *Journal of Physics A: Mathematical and Theoretical*, 2023. 2

[32] C. Liu, Y. Sun, Y. Xu, Z. Sun, X. Zhang, L. Lei, and G. Kuang. A review of optical and sar image deep feature fusion in semantic segmentation. *IEEE Journal of Selected Topics in Applied Earth Observations and Remote Sensing*, 2024. 2

[33] S. Mitra, S. Roy, and S. Hore. Assessment and forecasting of the urban dynamics through lulc based mixed model: evidence from agartala, india. *GeoJournal*, 88(2):2399–2422, 2023. 3

[34] Z. Ni, S. Li, X. Deng, Y. Cai, L. Zhang, W. Wang, Z.-B. Yang,

H. Yu, F. Yan, S. Liu, et al. Beating the break-even point with a discrete-variable-encoded logical qubit. *Nature*, 616(7955):56–60, 2023. 2

[35] M. A. Nielsen, I. Chuang, and L. K. Grover. *Quantum Computation and Quantum Information*, 2002. 2

[36] Y. Ouyang and E. T. Campbell. Trade-offs on number and phase shift resilience in bosonic quantum codes. *IEEE Transactions on Information Theory*, 67(10):6644–6652, 2021. 2

[37] A. Plotnitsky. The no-cloning life: Uniqueness and complementarity in quantum and quantum-like theories. *Entropy*, 25(5):706, 2023. 2

[38] P. Prasad, V. J. Loveson, P. Chandra, and M. Kotha. Evaluation and comparison of the earth observing sensors in land cover/land use studies using machine learning algorithms. *Ecological Informatics*, 68:101522, 2022. 3, 7

[39] V. Rajesh, U. P. Naik, et al. Quantum convolutional neural networks (qcnn) using deep learning for computer vision applications. In *2021 International conference on recent trends on electronics, information, communication & technology (RTEICT)*, pages 728–734. IEEE, 2021. 2

[40] A. Sebastianelli, D. A. Zaidenberg, D. Spiller, B. L. Saux, and S. L. Ullo. On Circuit-Based hybrid quantum neural networks for remote sensing imagery classification. *IEEE Journal of Selected Topics in Applied Earth Observations and Remote Sensing*, 15:565–580, 2022. 3, 7

[41] R. U. Shaik and S. Periasamy. Accuracy and processing speed trade-offs in classical and quantum svm classifier exploiting prisma hyperspectral imagery. *International Journal of Remote Sensing*, 43(15-16):6176–6194, 2022. 2

[42] Y. Shee, P.-K. Tsai, C.-L. Hong, H.-C. Cheng, and H.-S. Goan. Qubit-efficient encoding scheme for quantum simulations of electronic structure. *Physical Review Research*, 4(2):023154, 2022. 2

[43] N. L. Spong, Y. Jiao, O. D. Hughes, K. J. Weatherill, I. Lesanovsky, and C. S. Adams. Collectively encoded rydberg qubit. *Physical Review Letters*, 127(6):063604, 2021. 2

[44] M. Swathi and B. Rudra. Implementation of reversible logic gates with quantum gates. In *2021 IEEE 11th Annual Computing and Communication Workshop and Conference (CCWC)*, pages 1557–1563, Jan. 2021. 1

[45] M. Swathi and B. Rudra. An efficient approach for quantum entanglement purification. *International Journal of Quantum Information*, 20(04):2250004, 2022. 2

[46] M. Swathi and B. Rudra. Novel encoding method for quantum error correction. In *2022 IEEE 12th Annual Computing and Communication Workshop and Conference (CCWC)*, pages 1001–1005, Jan. 2022. 1

[47] B. Tan, M.-A. Lemonde, S. Thanasilp, J. Tangpanitanon, and D. G. Angelakis. Qubit-efficient encoding schemes for binary optimisation problems. *Quantum*, 5:454, 2021. 3

[48] A. Thomasberger, M. M. Nielsen, M. R. Flindt, S. Pawar, and N. Svane. Comparative assessment of five machine learning algorithms for supervised object-based classification of submerged seagrass beds using high-resolution uas imagery. *Remote Sensing*, 15(14):3600, 2023. 3, 7

[49] N. Thumwanit, C. Lortaraprasert, and R. Raymond. Invited: Trainable discrete feature embeddings for quantum machine learning. In *2021 58th ACM/IEEE Design Automation Conference (DAC)*, pages 1352–1355, Dec. 2021. 2

[50] A. Tiwari, S. K. Sharma, A. Dixit, and V. Mishra. Uav remote sensing for campus monitoring: a comparative evaluation of nearest neighbor and rule-based classification. *Journal of the Indian Society of Remote Sensing*, 49(3):527–539, 2021. 3

[51] Y.-L. Wei, Y.-B. Zheng, R. Wang, and H.-C. Li. Quaternion convolutional neural network with emap representation for multisource remote sensing data classification. *IEEE Geoscience and Remote Sensing Letters*, 2023. 2, 7

[52] Q. Xu, G. Zheng, Y.-X. Wang, P. Zoller, A. A. Clerk, and L. Jiang. Autonomous quantum error correction and fault-tolerant quantum computation with squeezed cat qubits. *npj Quantum Information*, 9(1):78, 2023. 2